

DRP schemes perform poorly for decaying or growing oscillations

Edward J. Brambley,*

DAMTP, Cambridge CB3 0WA, UK

Computational aeroacoustics often uses high-order finite difference schemes optimized to require relatively few points per wavelength; such optimized schemes are often called Dispersion Relation Preserving (DRP). Here we ask the question: what is the equivalent of points per wavelength for growing or decaying waves, and how well are such waves resolved numerically? This paper shows that DRP optimized spatial derivatives perform poorly for waves that are not of constant amplitude, under performing maximal-order schemes. Such non-constant-amplitude waves are common in aeroacoustics, whether owing to the $O(1/r)$ decay of an expanding spherical wave, due to exponential decay caused by acoustic linings, or because of the decay of high-azimuthal-order modes in the radial direction towards the centre of a cylindrical duct. An equivalent criterion to points per wavelength is proposed for non-constant-amplitude oscillations, reducing to the standard definition for constant-amplitude oscillations and valid even for pure growth or decay with no oscillation. Using this definition, coherent statements about points per wavelength necessary for a given accuracy can be made for maximum-order schemes applied to non-constant-amplitude oscillations. These features are illustrated through a numerical example.

I. Introduction

Computational aeroacoustics often uses high-order finite difference schemes optimized to need relatively few points per wavelength. Given a series of equidistant points $x_j = j\Delta x$ and function evaluations $f_j = f(x_j)$, an explicit symmetric scheme numerically approximates the derivative $f'(x_j)$ by

$$f'_j = \frac{1}{\Delta x} \sum_{q=1}^N d_q (f_{j+q} - f_{j-q}). \quad (1)$$

For such schemes, a function $f(x) = Ae^{i\alpha x}$ with derivative $f'(x) = i\alpha Ae^{i\alpha x}$ gives a numerical derivative

$$f'_j = i\bar{\alpha} Ae^{i\alpha x_j}, \quad \text{where} \quad \bar{\alpha}\Delta x = 2 \sum_{q=1}^N d_q \sin(\alpha\Delta x q). \quad (2)$$

Equation (2) represents the harmonic behaviour of the differentiation scheme. A classical choice of d_q is to give as accurate as possible a derivative in the limit $\Delta x \rightarrow 0$. This choice would give $f'_0 = f'(0) + O((\Delta x)^{2N})$, and such $2N$ th order schemes are referred to here as maximal-order schemes. An alternative is to specify that $f'_0 = f'(0) + O((\Delta x)^{2L})$, and to use the remaining $N - L$ degrees of freedom to optimize the derivative such that $\bar{\alpha}$ is as close to α as possible under some suitable metric. For example, Tam & Webb¹ chose $N = 3$ and $L = 2$ and optimized the remaining coefficient to minimize

$$\int_0^\eta (\bar{\alpha}\Delta x - \alpha\Delta x)^2 d(\alpha\Delta x) \quad (3)$$

with $\eta = \pi/2$, while Tam & Shen² subsequently suggested $\eta = 1.1$ gives a more balanced scheme. These optimized results are often presented as in figure 1.

The idea of analysing the harmonic behaviour of numerical derivatives in this way dates back at least to Vichnevetsky & De Schutter⁵ and is discussed in detail by Vichnevetsky & Bowles⁶, while Holberg⁷ considered schemes based on optimizing the numerical group velocity. Lele⁸ considered the harmonic accuracy

*Royal Society University Research Fellow, Department of Applied Mathematics & Theoretical Physics, University of Cambridge, CMS, Wilberforce Road, Cambridge CB3 0WA, United Kingdom. AIAA senior member.

Copyright © 2015 by E.J. Brambley. Published by the American Institute of Aeronautics and Astronautics, Inc. with permission.

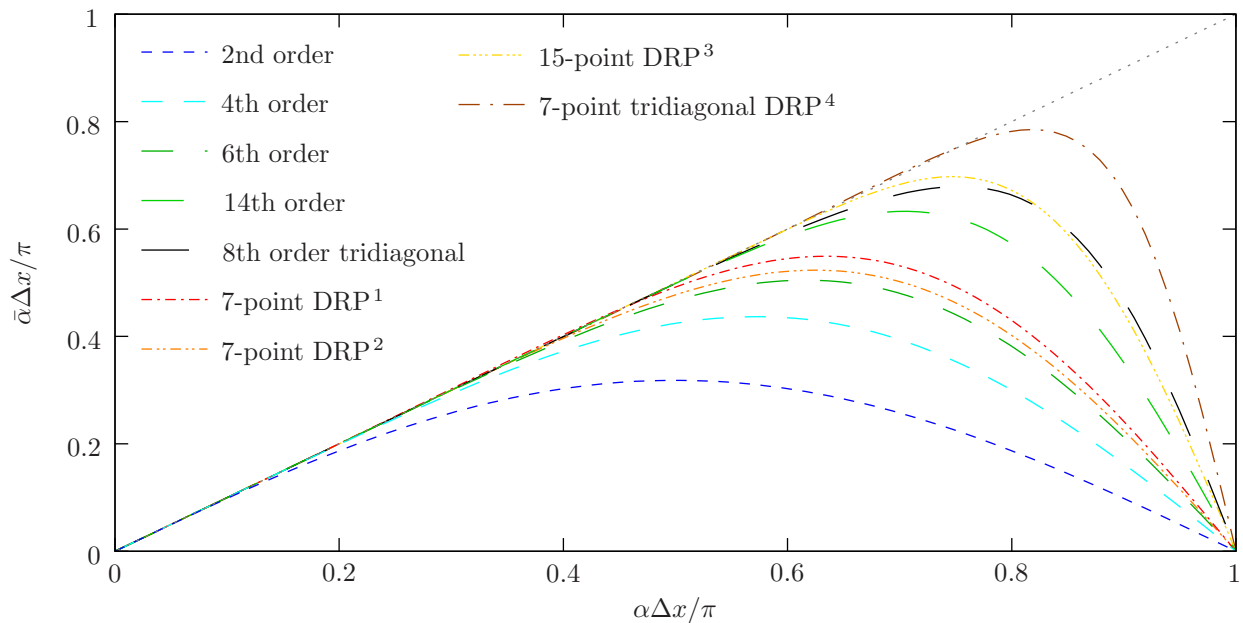


Figure 1. Graph of the effective numerical wavenumber $\bar{\alpha}$ when calculating the derivative of a wave with actual wavenumber α using a finite-difference scheme with points separated by Δx . The 2nd, 4th, 6th and 14th order schemes are the standard explicit maximum-order schemes involving 3, 5, 7, and 15 point stencils respectively, while the 8th order tridiagonal implicit scheme uses a 7-point stencil. All DRP schemes are optimized subject to being 4th order. DRP¹ is optimized for $|\alpha\Delta x/\pi| < 0.5$ while DRP² is optimized for $|\alpha\Delta x/\pi| < 0.35$

of implicit stencils, which were subsequently optimized by Kim & Lee⁴. Optimized schemes were termed “spectral-like” by Lele⁸, “maximum resolution” by Kim & Lee⁴, and “extended wavenumber” by Zingg & Lomax⁹, while Tam & Webb¹ coined the term Dispersion Relation Preserving (DRP). This analysis spurred further investigations, including into 2D spatial derivatives on triangular grids by Zingg & Lomax⁹, into larger width optimized stencils by Bogey & Bailly¹⁰, into non-equidistant grids by Jakobsson¹¹, and into anisotropic effects on 2D grids with convection by Chenoweth, Soria & Ooi¹², to name but a few. The field is still being actively investigated, for example by Zhang & Yao¹³ using sup-norms and a simulated annealing optimization algorithm, and is regularly rediscovered, as for example by Liu¹⁴ in the geophysics context. For further details, see the excellent comparison by Zingg¹⁵, the review by Astley¹⁶, and the recent book by Tam³.

Optimized DRP schemes are designed to require fewer points per wavelength for accurate resolution of waves. The present paper is partially motivated by the question: what is the equivalent of points per wavelength for exponentially growing or decaying waves, and how well are such waves resolved numerically? Exponential growth or decay is often found in aeroacoustics, either due to acoustic linings that cause an exponential decrease in amplitude as a wave propagates along the lining, or due to the natural decay in the radial direction from wall to centreline of a high-order spinning mode in a cylindrical duct (such as is commonly excited by an aeroengine rotor). Surface waves over acoustic linings also exhibit exponential decay in the direction normal to the lining^{17–19}, while weaker decay is often found due to the $O(1/r)$ decay of a spherical wavefront, which can be rather quick in the vicinity of a point source generating such a spherical wave.

As an example, Tam, Ju & Chien²⁰ considered the effect of liner splices on the decay of an upstream-propagating wave in a cylindrical duct for aeroacoustically-relevant parameters. In nondimensional terms, the axial wavenumber they needed to resolve was $\alpha = -14.7 + 7.6i$ in the no-flow case and $\alpha = -21.0 + 12.0i$ in the case with flow. In both of these cases, the spatial wavenumber clearly has a significant imaginary part, and it is unclear how figure 1 applies in such situations; this is the topic of this paper.

II. Non-constant amplitude harmonic analysis

Here we consider oscillations that grow or decay as well as oscillating. Such oscillations are characterized by a wavenumber α that is complex; this is the novel insight of this paper. While what follows is equally valid for any finite difference scheme on any grid, here for simplicity we consider only symmetric finite difference schemes on regularly spaced grids. We will, however, consider both implicit (i.e. compact) and explicit finite difference schemes, so that our derivatives are given by

$$f'_j + \sum_{q=1}^M \beta_q (f'_{j+q} + f'_{j-1}) = \frac{1}{\Delta x} \sum_{q=1}^N d_q (f_{j+q} - f_{j-q}) \quad \Rightarrow \quad \bar{\alpha} \Delta x = \frac{2 \sum_{q=1}^N d_q \sin(\alpha \Delta x q)}{1 + 2 \sum_{q=1}^M \beta_q \cos(\alpha \Delta x q)}. \quad (4)$$

For $M = 0$ this reduces to the explicit (i.e. non-compact) scheme given in (1) and (2) above, with f'_j determined explicitly in terms of f_{j+q} . The $M = 1$ and $M = 2$ cases are referred to as tridiagonal and pentadiagonal implicit schemes respectively.

A. Performance of optimized and maximal-order schemes for non-constant-amplitude waves

Equation (4) still holds even for complex α . Considering first the relative phase error $\varepsilon_p = |\bar{\alpha}/\alpha - 1|$, for several explicit schemes ε_p is plotted in figure 2. As can be seen, the classical maximum-order schemes perform better than the optimized DRP schemes when $\text{Im}(\alpha) \neq 0$. This is not surprising, since the DRP schemes have been optimized to give a good approximation only for real α and we now see this is at the expense of behaviour for complex α . A similar situation is seen in figure 3 for implicit schemes.

B. Comparison of optimized and maximal-order schemes for non-constant-amplitude waves

Possibly a more relevant summary is to consider which of the maximal-order or DRP schemes is more accurate for a given α . This is plotted (for values of α for which at least one scheme gives at least 1% relative accuracy) for the relative phase error ε_p in figure 4 for explicit schemes, and in figure 5 for implicit schemes. The region of α for which the optimized DRP schemes are more accurate than the classical maximum-order schemes can be seen to be rather limited in both cases. Several other schemes have been investigated, including those based on trigonometric interpolation by Tang & Baeder²¹, and similar results to those presented here are seen in all cases considered. In all cases, and for any resolution Δx , the optimized schemes are seen to give worse phase accuracy than the maximum-order schemes for the parameters simulated by Tam, Ju & Chien²⁰.

The same is true when the relative group velocity error is considered. The relative group velocity is given by differentiating (4),

$$\frac{d\bar{\alpha}}{d\alpha} = \frac{\left(\sum_{q=1}^N q d_q \cos(\alpha \Delta x q)\right) \left(1 + \sum_{q=1}^M \beta_q \cos(\alpha \Delta x q)\right) + \left(\sum_{q=1}^N d_q \sin(\alpha \Delta x q)\right) \left(\sum_{q=1}^M q \beta_q \sin(\alpha \Delta x q)\right)}{\left(1 + \sum_{q=1}^M \beta_q \cos(\alpha \Delta x q)\right)^2}. \quad (5)$$

We define the relative group velocity error following Trefethen²² and Holberg⁷ as $\varepsilon_g = |d\bar{\alpha}/d\alpha - 1|$. Similar plots to figures 4 and 5 are plotted in figures 6 and 7. The original DRP scheme of Tam & Webb¹ and each of the optimized tri-diagonal implicit schemes can be seen to fare particularly poorly with respect to the group velocity error.

C. A points-per-wavelength equivalent for non-constant-amplitude waves

Figures 2 and 3 suggest that, for maximal order schemes, the accuracy depends on $|\alpha \Delta x|$ but is insensitive to $\arg(\alpha \Delta x)$ at least for small $|\alpha \Delta x|$. Hence, the equivalent of points per wavelength for non-constant-amplitude waves is suggested here to be $\text{PPW} = 2\pi/|\alpha \Delta x|$, which reduces to the usual definition when α is real. Using this definition, a certain accuracy can be guaranteed for a certain number of points per wavelength if a maximum-order scheme is used. This definition is however not helpful for DRP schemes, since their accuracy depends both on $|\alpha \Delta x|$ and $\arg(\alpha \Delta x)$. It is therefore proposed here that, unless specific a priori knowledge of the exact wavenumbers present in *all* directions (e.g. axial, radial and azimuthal directions for waves in a cylinder) are known, computational simulations are likely to be more accurate using the classical maximum-order schemes than using optimized DRP schemes.

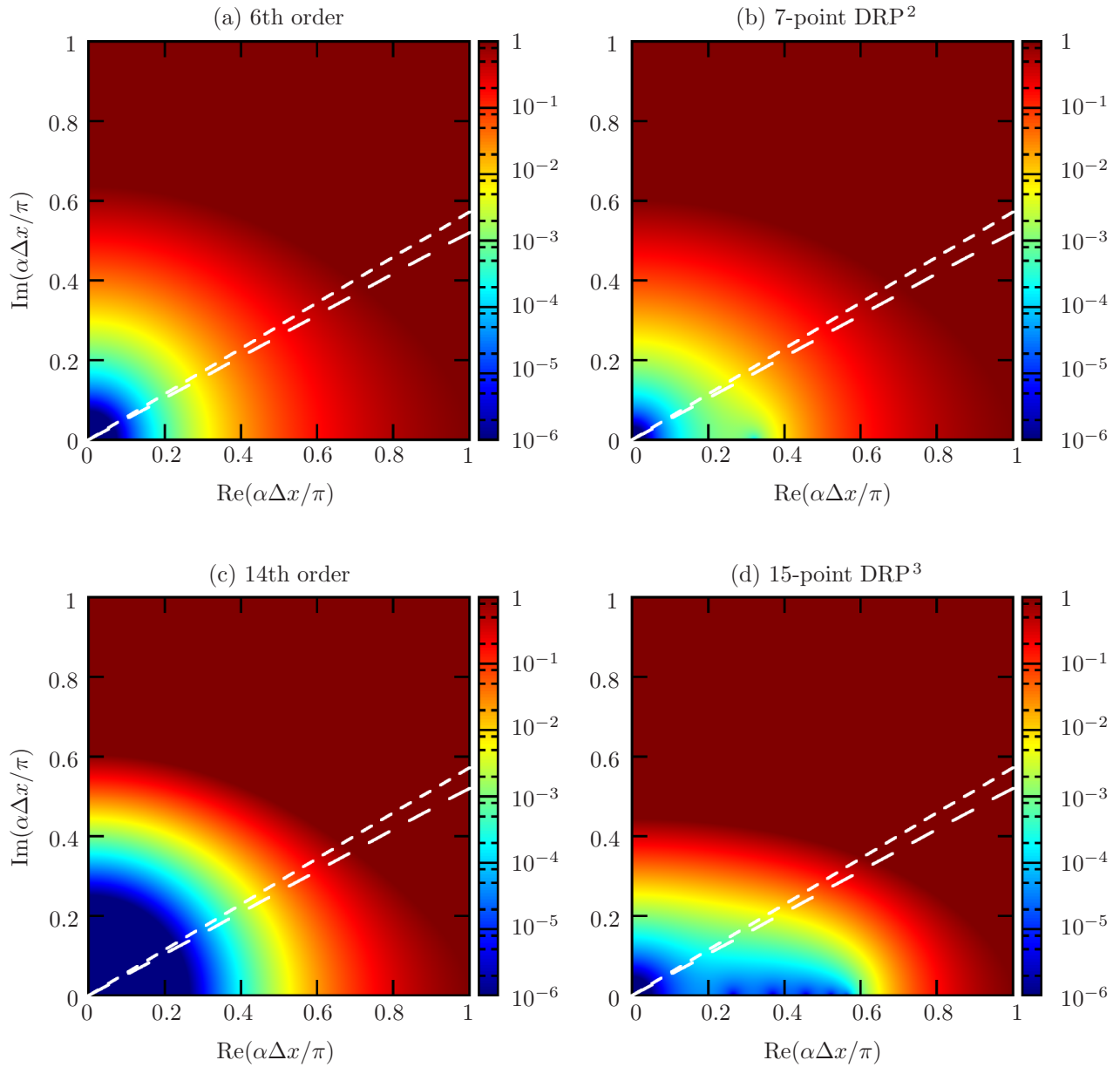


Figure 2. For explicit schemes, plots of $|\bar{\alpha}/\alpha - 1|$ for complex α on a logarithmic scale, giving the relative accuracy of the numerical derivative. (a) and (b) use 7-point stencils, while (c) and (d) use 15-point stencils. (a) and (c) are maximum-order schemes, while (b) and (d) are optimized 4th order schemes. Short and long dashed lines correspond to $\alpha\Delta x$ for varying Δx with and without flow respectively for the axial wavenumbers investigated by Tam, Ju & Chien²⁰.

One obvious class of a priori knowledge would be if waves were known to be of constant amplitude. This is unlikely in practice, but unfortunately it is common to test DRP schemes by solving the 1D advection equation

$$\frac{\partial f}{\partial t} + \frac{\partial f}{\partial x} = 0, \quad (6)$$

for which waves do propagate with constant amplitude. This helps explain why flaws in optimized DRP schemes for non-constant-amplitude oscillations have not been demonstrated previously. A test case involving non-constant-amplitude oscillations is given in the next section.

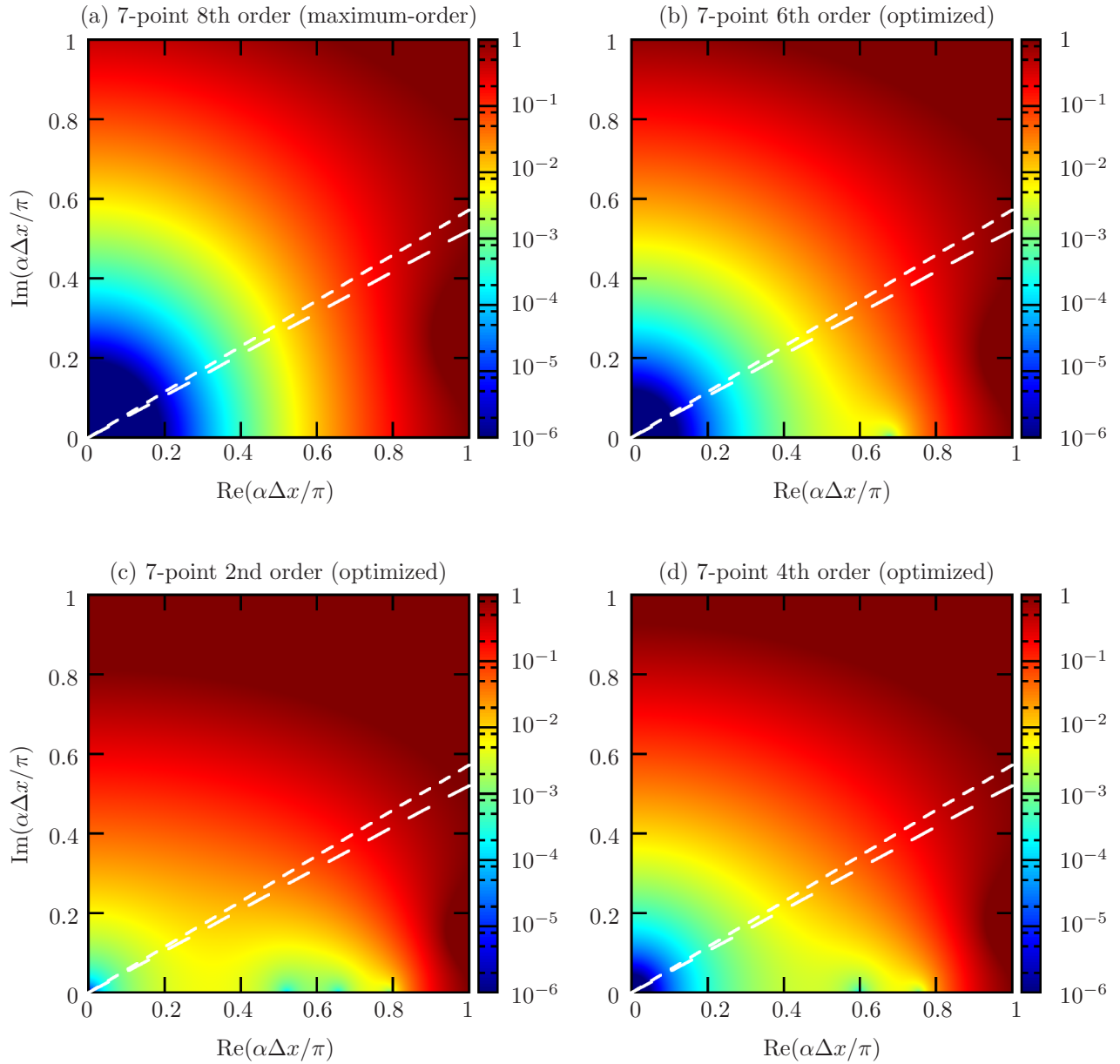


Figure 3. Plots of $|\tilde{\alpha}/\alpha - 1|$ for complex α on a logarithmic scale, giving the relative accuracy of the numerical derivative, for tri-diagonal implicit 7-point schemes from Kim & Lee⁴. Short and long dashed lines correspond to $\alpha\Delta x$ for varying Δx with and without flow respectively for the axial wavenumbers investigated by Tam, Ju & Chien²⁰.

III. Numerical Demonstration

In this section, a rather basic numerical example is given to illustrate the theory mentioned above. In order to avoid the complication of mixing spatial and temporal derivatives, but remaining relevant to aeroacoustic applications, we here consider numerical solutions of the Pridmore-Brown equation²³, given by

$$\frac{d^2 p}{dr^2} + \left(\frac{2\alpha U'}{\omega - U\alpha} + \frac{1}{r} - \frac{\rho'}{\rho} \right) + \left((\omega - U\alpha)^2 \rho - \alpha^2 - \frac{m^2}{r^2} \right) p = 0, \quad \text{subject to } p(0) \neq \infty, \quad (7)$$

where $U(r)$ and $\rho(r)$ are the velocity and density of the mean flow normalized by the centreline sound speed and density respectively, ω is the Helmholtz number, α is the nondimensionalized axial wavenumber and m is the azimuthal wavenumber. Even when U and ρ are constant, for which (7) reduces to Bessel's equation

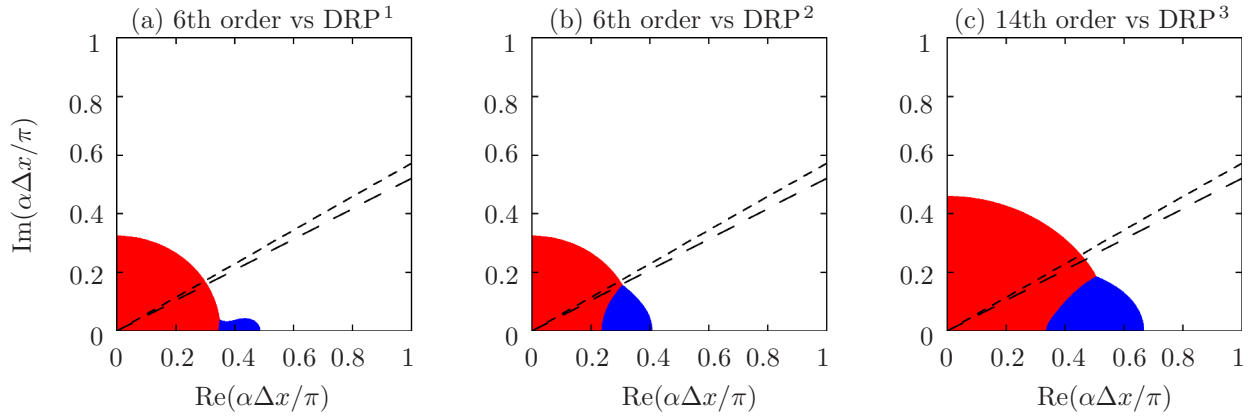


Figure 4. Comparison, for complex wavenumbers α , showing where the maximum-order (red) or DRP (blue) scheme is most accurate. White areas indicate regions where neither scheme is within 1% accuracy (i.e. $|\bar{\alpha}/\alpha - 1| > 0.01$). (a) and (b) are 7-point explicitly schemes, while (c) is a 15-point explicit scheme. All DRP schemes are optimized subject to 4th order accuracy. Short and long dashed lines correspond to $\alpha\Delta x$ for varying Δx with and without flow respectively for the axial wavenumbers investigated by Tam, Ju & Chien²⁰.

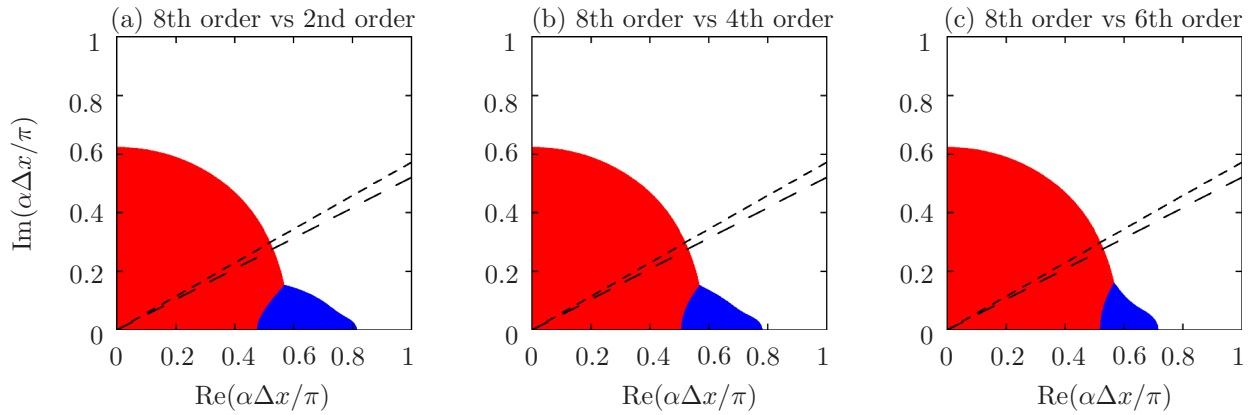


Figure 5. Comparison, for complex wavenumbers α , showing which of the maximum-order (8th order, red) or maximum-resolution (optimized, blue) 7-point tri-diagonal implicit schemes is most accurate. Optimized schemes are taken from Kim & Lee⁴. White areas indicate regions where neither scheme is within 1% accuracy (i.e. $|\bar{\alpha}/\alpha - 1| > 0.01$). Short and long dashed lines correspond to $\alpha\Delta x$ for varying Δx with and without flow respectively for the axial wavenumbers investigated by Tam, Ju & Chien²⁰.

with exact explicit solution

$$p = J_m(r\sqrt{(\omega - U\alpha)^2 - \alpha^2}\rho), \quad (8)$$

this equation still exhibits oscillations with rapid variations in amplitude, and if a thin boundary layer is introduced into $U(r)$ and $\rho(r)$ then even more dramatic amplitude variations are possible (e.g. figure 1 of Ref. 24). Moreover, since this equation models the radial distribution of wave modes in a cylindrical duct, it has several features in common with the equations being solved in the radial direction in time-domain CAA.

Numerical solutions will be sought to (7) through the auxiliary variable $\xi(r)$, where

$$\xi(r) = \frac{r(\omega - M\alpha) dp}{\rho(\omega - U\alpha)^2 dr} \quad \Rightarrow \quad \begin{aligned} \xi' + r(\omega - M\alpha) \left[1 - \frac{\alpha^2 + m^2/r^2}{\rho(\omega - U\alpha)^2} \right] p &= 0 \\ p' - \frac{\rho(\omega - U\alpha)^2}{r(\omega - M\alpha)} \xi &= 0 \end{aligned} \quad (9)$$

where $M = U(0)$. At $r = 0$ we specify $p(0) = 0$ if $m \neq 0$ or $\xi'(0) = 0$ if $m = 0$, and in either case we also specify that $\xi(0) = 0$. At $r = 1$ we specify $p(1) = 1$ to force a non-zero solution. We discretize

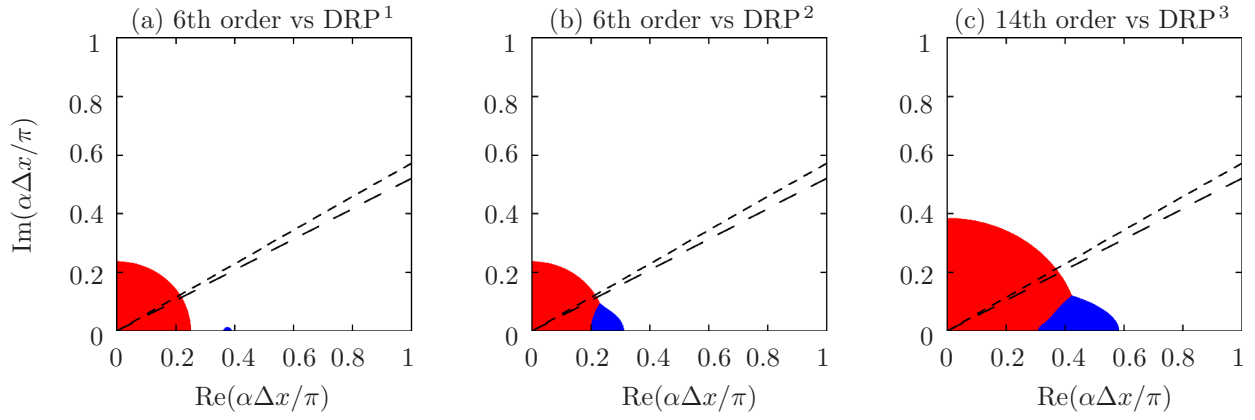


Figure 6. Comparison, for complex wavenumbers α , showing where the maximum-order (red) or DRP (blue) scheme is most accurate according to the relative group velocity error ε_g . White areas indicate regions where neither scheme is within 1% accuracy (i.e. $|\frac{d\bar{\alpha}}{d\alpha} - 1| > 0.01$). (a) and (b) are 7-point explicitly schemes, while (c) is a 15-point explicit scheme. All DRP schemes are optimized subject to 4th order accuracy. Short and long dashed lines correspond to $\alpha\Delta x$ for varying Δx with and without flow respectively for the axial wavenumbers investigated by Tam, Ju & Chien²⁰.

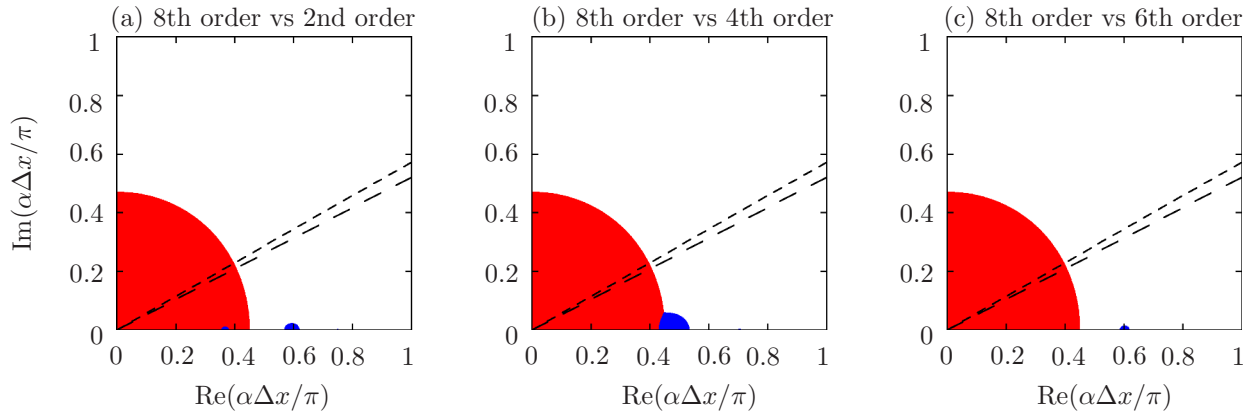


Figure 7. Comparison, for complex wavenumbers α , showing which of the maximum-order (8th order, red) or maximum-resolution (optimized, blue) 7-point tri-diagonal implicit schemes is most accurate according to the relative group velocity error ε_g . Optimized schemes are taken from Kim & Lee⁴. White areas indicate regions where neither scheme is within 1% accuracy (i.e. $|\frac{d\bar{\alpha}}{d\alpha} - 1| > 0.01$). Short and long dashed lines correspond to $\alpha\Delta x$ for varying Δx with and without flow respectively for the axial wavenumbers investigated by Tam, Ju & Chien²⁰.

the interval $[0, 1]$ with $N + 1$ equally spaced points, and write our $2N + 2$ degrees of freedom as $\mathbf{v} = (p_0, \xi_0, p_1, \xi_1, \dots, p_N, \xi_N)$. Then discretizing (9) and using the implicit derivative scheme (4) gives

$$\begin{aligned} \mathbf{v}' &= \mathbf{L}\mathbf{v} + \mathbf{q} \\ \mathbf{B}\mathbf{v}' &= \frac{1}{\Delta x}\mathbf{D}\mathbf{v} \end{aligned} \quad \Rightarrow \quad (\mathbf{B}\mathbf{L} - \frac{1}{\Delta x}\mathbf{D})\mathbf{v} = -\mathbf{B}\mathbf{q}, \quad (10)$$

where \mathbf{B} is a banded matrix consisting of the β_j coefficients (and is the identity for an explicit scheme), \mathbf{D} is a banded matrix consisting of the d_j coefficients, and \mathbf{q} has only one nonzero element forcing the boundary condition $p(1) = 1$. Suitable asymmetric or reduced-width stencils are needed at the edges of the domain; here, we use explicit stencils at the boundaries for stability, and choose them to be of very high order to ensure that the global error is dominated by the symmetric stencils of interest within the domain, rather than coming from the boundaries.

In order to compare with the analytic Bessel's function solution (8), we take $U(r) = M$ constant and $\rho(r) = 1$. Since the solution is already normalized such that $p(1) = 1$, the maximum absolute error $\mathcal{E} = \max_{j=0}^N \{p_j - p(j\Delta x)\}$ is plotted in what follows. Figure 8(a) shows how the absolute error \mathcal{E} varies with number of points N for the 7-point explicit DRP and maximal order schemes, for parameters typical of an

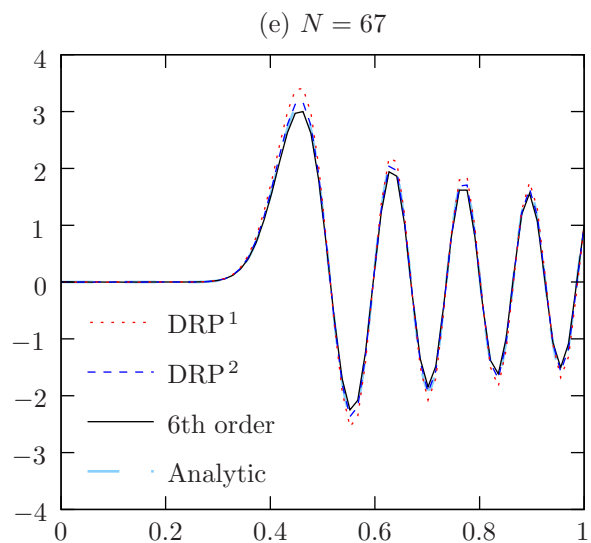
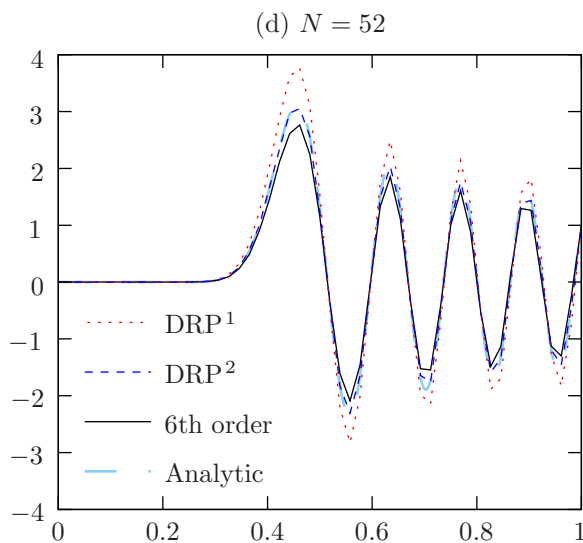
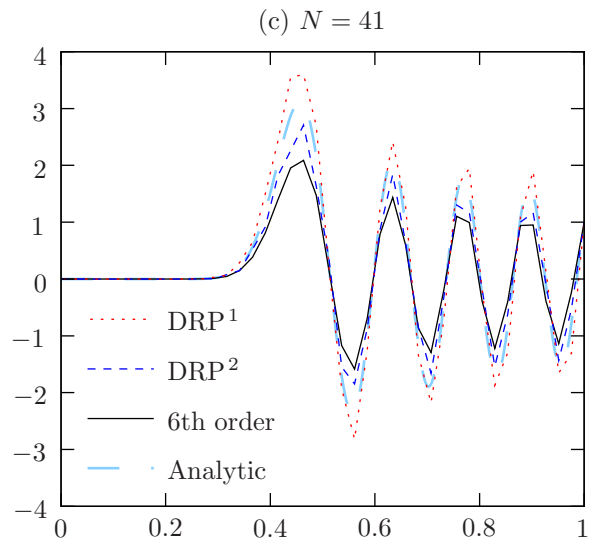
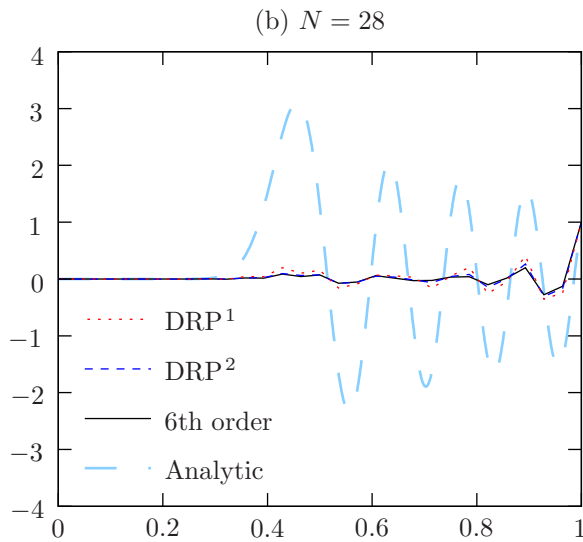
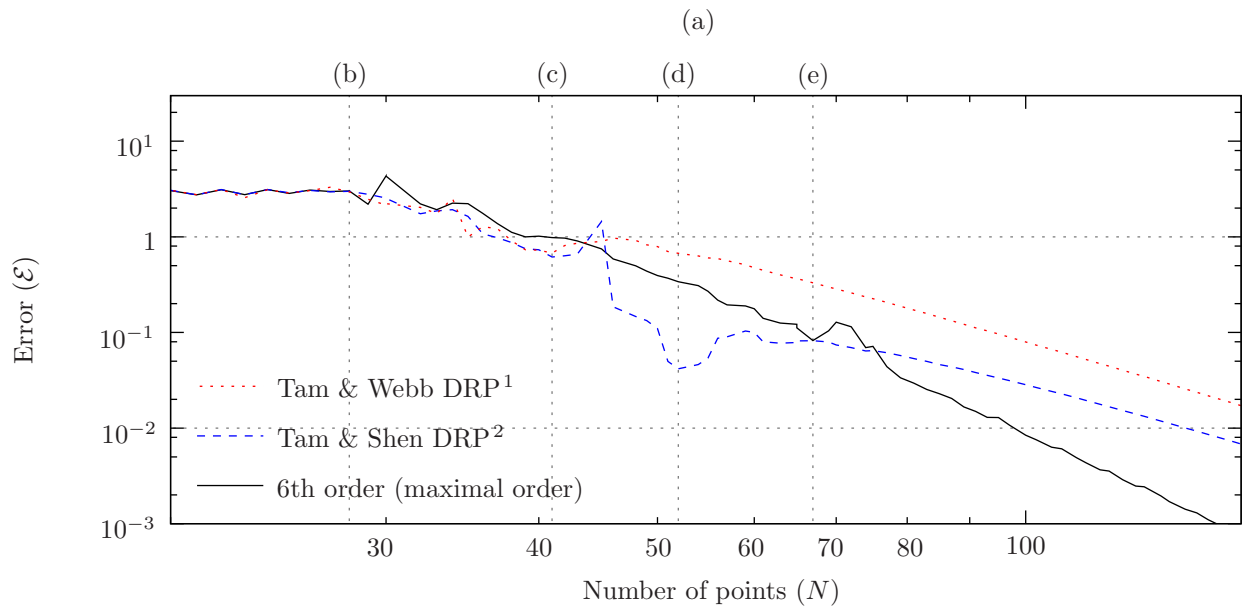


Figure 8. Comparison of the analytic solution and numerical solutions to (10) for various numbers of points N , for 7-point explicit finite-difference stencils. $\omega = 50$, $m = 24$, $M = 0.5$, and $k = -35$, representing a typical aeroacoustic mode near cut-off.

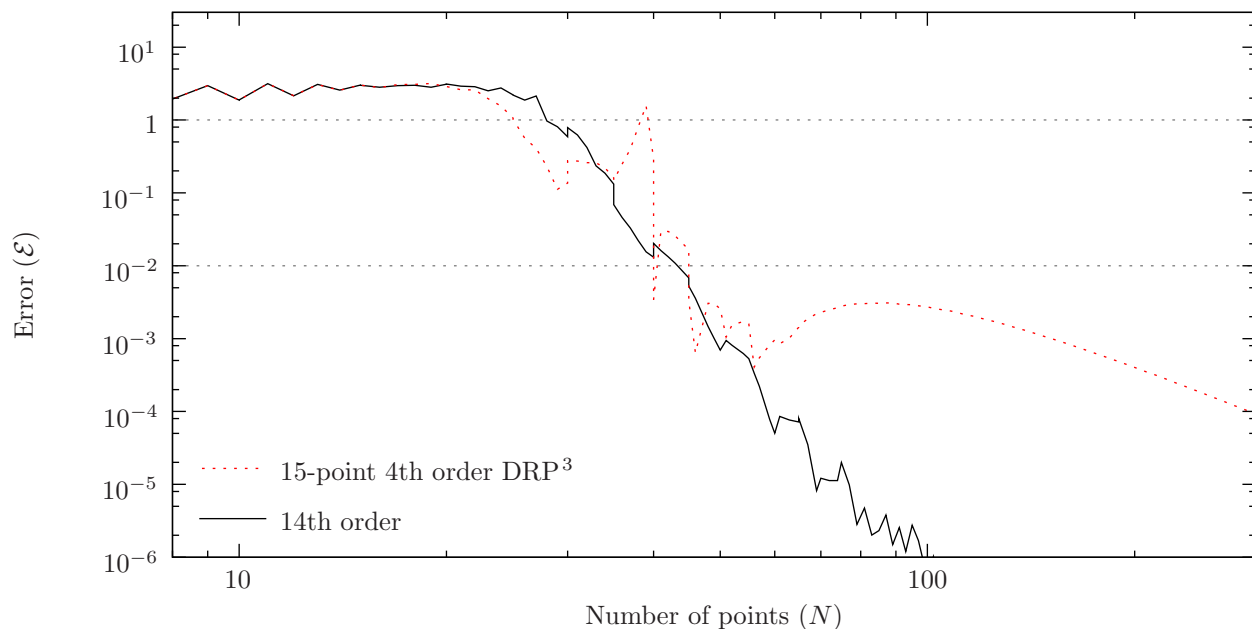


Figure 9. Absolute error solving Bessel’s equation (10) with N points in the interval $r \in [0, 1]$ using the given 15-point explicit finite-difference stencils. $\omega = 50$, $m = 24$, $M = 0.5$, and $k = -35$, representing a typical aeroacoustic mode near cut-off.

aeroengine rotor-alone tone near cut-off. Since this is a 9th radial-order mode, it is quite highly oscillatory (see figure 8(e)), and so DRP schemes might be expected to perform substantially better than non-optimized schemes in this case. Plots of $p(r)$ for four different grids are given in figure 8(b–e). For small N no scheme correctly resolves the solution, and the error is greater than one. The heavily optimized Tam & Webb DRP scheme¹ has a local minimum in the error at around $N = 41$ (c), though this is not enough to accurately resolve the solution and the error remains above 50%. The more balanced DRP scheme of Tam & Shen² has a far more pronounced local minimum at around $N = 52$ (d); while this local minimum gives a reasonable looking agreement in figure 8(d), the maximum absolute error \mathcal{E} shows the solution does no better than 4% accuracy, and moreover for finer grids than this the error returns to a clearly unacceptable 10% until the grid becomes much finer. In order to obtain 1% accuracy $N \geq 99$ is needed in this case, and this is achieved first by the maximum order stencil. Clearly, the DRP schemes are only worth using in their “sweet spot” around their local error minima, which are rather narrow, and therefore significant a priori knowledge is needed.

Figure 9 shows the \mathcal{E} against N curves for two 15-point explicit stencils, a 4th order DRP stencil³ and a maximum order stencil. For these stencils, 1% accuracy is obtained for $N \geq 45$, and both optimized and maximal order stencils achieve this almost simultaneously. Put another way, the DRP scheme shows no advantage over the maximal order scheme in this case.

Figure 10 shows a similar plot for the tri-diagonal implicit 7-point schemes of Kim & Lee⁴. For errors less than 10%, no advantage is provided by the optimized schemes over the maximal order scheme.

While this section has considered only one set of parameters, a number of other parameters have been tried and rather similar results observed. Indeed, in cases with less oscillation the maximum order schemes are observed to perform even better compared to the optimized schemes.

IV. Conclusion

We have reconsidered the rather classical theory of the harmonic behaviour of finite difference stencils, where a wave with actual wavenumber α gives a numerical derivative with an effective numerical wavenumber $\bar{\alpha}$. Here, we no longer restrict α to be real; non-real α corresponds to exponentially growing or decaying waves, which it is argued are ubiquitous in aeroacoustics. Finite difference stencils that have been optimized over real α are shown to perform worse for complex α than maximal order stencils, for which no such assumption of real α has been made. This is of course unsurprising, and it is possible that stencils could be

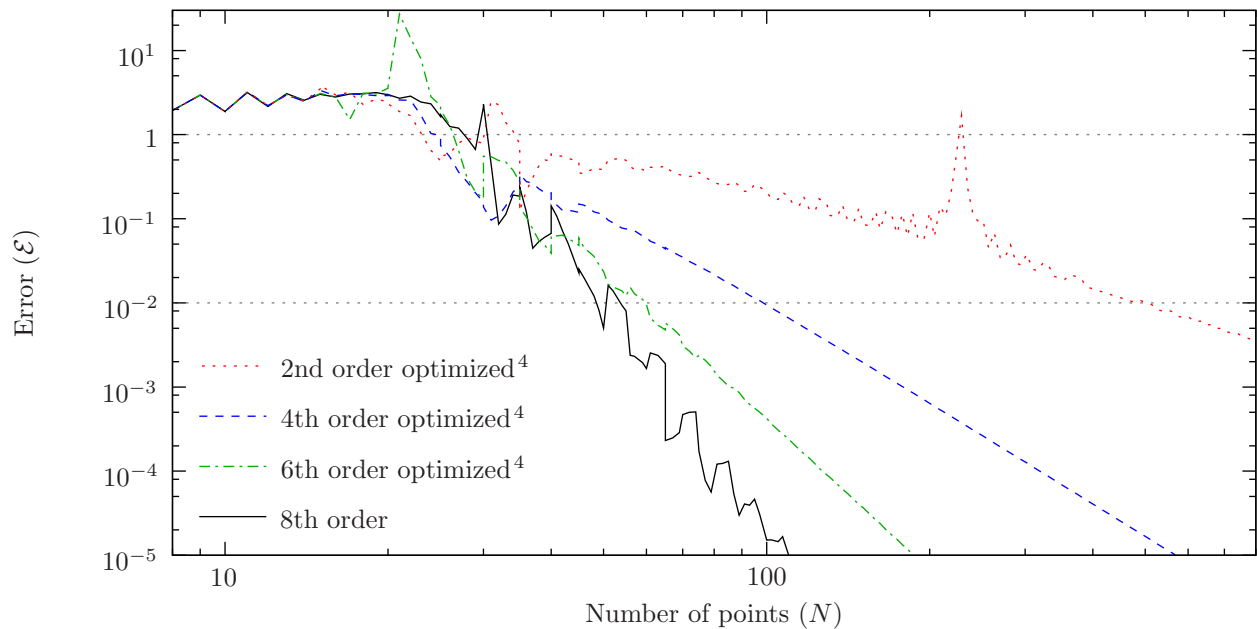


Figure 10. Absolute error solving Bessel’s equation (10) with N points in the interval $r \in [0, 1]$ using tri-diagonal implicit 7-point stencils from Kim & Lee⁴. $\omega = 50$, $m = 24$, $M = 0.5$, and $k = -35$, representing a typical aeroacoustic mode near cut-off.

optimized over a range of complex α ; this optimization has not been attempted here.

The accuracy of maximal order stencils appears to depend strongly on $|\alpha\Delta x|$ but rather weakly if at all on $\arg(\alpha\Delta x)$, at least for small $|\alpha\Delta x|$, as can be seen in figures 2 and 3. Hence, an equivalent of points per wavelength for non-constant-amplitude waves is suggested here to be $PPW = 2\pi/|\alpha\Delta x|$, which reduces to the usual definition when α is real. Using this definition, a certain accuracy can be guaranteed for a certain number of points per wavelength if a maximum-order scheme is used. This definition is however not helpful for DRP schemes, since their accuracy depends both on $|\alpha\Delta x|$ and $\arg(\alpha\Delta x)$.

As a single numerical example to illustrate this behaviour, solutions to the Pridmore-Brown equation have been sought. This equation has non-constant-amplitude oscillatory solutions, and is typical of CAA solutions in the radial direction for cylindrical duct acoustics. Even for the significantly oscillatory solution considered, optimized DRP schemes performed poorly relative to maximal order schemes due to the non-constant-amplitude oscillations. The DRP schemes do have a “sweet spot” with reasonable behaviour, but this is often rather narrow and neighbouring resolutions have poor accuracy of worse than 10% in the case considered. Even in the sweet spot the accuracy was no better than 4% for the case considered. It is therefore suggested here that, unless significant a priori knowledge of the exact wavenumbers present in *all* directions is available (e.g. in the axial, radial and azimuthal directions for waves in a cylinder), computational simulations are likely to be more accurate using the classical maximum-order schemes than using optimized DRP schemes. In particular, one of the advantages of time-domain CAA simulations is to consider broadband sound, in which case it is extremely unlikely that all relevant sources coincide with the same DRP sweet spot.

The optimized schemes also performed worse than the maximal order ones for non-constant-amplitude oscillations when the group error $|d\bar{\alpha}/d\alpha - 1|$ rather than phase error $|\bar{\alpha}/\alpha - 1|$ was considered. The group error is not relevant for the Pridmore-Brown example given here, since the Pridmore-Brown solution involves a matrix inversion (10) which is therefore nonlocal, and hence correct propagation of information at the group velocity is not tested. This suggests that the rather close behaviour of the 6th order (optimized) and 8th order (maximal order) tri-diagonal schemes shown in figure 10 might be misleading, as figure 7 shows that the 6th order scheme performs poorly at maintaining the correct group velocity compared with the maximal order scheme.

Further possibilities for future research include optimizing numerical derivatives over a range of *complex* wavenumbers, and investigating non-constant-amplitude oscillations on 2D grids or for temporal rather than spatial derivatives, or indeed for combined spatio-temporal schemes (e.g. Refs. 25,26).

References

- ¹ Tam, C. K. W. and Webb, J. C., “Dispersion-Relation-Preserving Finite Difference Schemes for Computational Acoustics,” *J. Comput. Phys.*, Vol. 107, 1993, pp. 262–281.
- ² Tam, C. K. W. and Shen, H., “Direct Computation of Nonlinear Acoustic Pulses using High-Order Finite Difference Schemes,” AIAA paper 93-4325, 1993.
- ³ Tam, C. K. W., *Computational Aeroacoustics*, chap. 2, Cambridge, 2012.
- ⁴ Kim, J. W. and Lee, D. J., “Optimized Compact Finite Difference Schemes with Maximum Resolution,” *AIAA J.*, Vol. 34, No. 5, 1996, pp. 887–893.
- ⁵ Vichnevetsky, R. and De Schutter, F., “A Frequency Analysis of Finite Element Methods for Initial Value Problems,” *Advances in Computer Methods for Partial Differential Equations*, edited by R. Vichnevetsky, AICA, Rutgers Univ., New Brunswick, NJ, 1975.
- ⁶ Vichnevetsky, R. and Bowles, J. B., *Fourier Analysis of Numerical Approximations of Hyperbolic Equations*, SIAM, Philadelphia, 1982.
- ⁷ Holberg, O., “Computational Aspects of the Choice of Operator and Sampling Interval for Numerical Differentiation in Large-Scale Simulation of Wave Phenomena,” *Geophysical Prospecting*, Vol. 35, 1987, pp. 629–655.
- ⁸ Lele, S. K., “Compact Finite Difference Schemes with Spectral-like Resolution,” *J. Comput. Phys.*, Vol. 103, 1992, pp. 16–42.
- ⁹ Zingg, D. W. and Lomax, H., “Finite-Difference Schemes on Regular Triangular Grids,” *J. Comput. Phys.*, Vol. 108, 1993, pp. 306–313.
- ¹⁰ Bogey, C. and Bailly, C., “A Family of Low Dispersive and Low Dissipative Explicit Schemes for Flow and Noise Computations,” *J. Comput. Phys.*, Vol. 194, 2004, pp. 194–214.
- ¹¹ Jakobsson, S., “Frequency Optimized Computation Methods,” *J. Sci. Comput.*, Vol. 26, 2006, pp. 329–362.
- ¹² Chenoweth, S. K. M., Soria, J., and Ooi, A., “A New Perspective on Spectral Analysis of Numerical Schemes,” *Int. J. Numer. Meth. Fluids*, Vol. 68, 2012, pp. 467–482.
- ¹³ Zhang, J.-H. and Yao, Z.-X., “Optimized Explicit Finite-Difference Schemes for Spatial Derivatives using Maximum Norm,” *J. Comput. Phys.*, Vol. 250, 2013, pp. 511–526.
- ¹⁴ Liu, Y., “Globally Optimal Finite-Difference Schemes based on Least Squares,” *Geophysics*, Vol. 78, No. 4, 2013, pp. T113–T132.
- ¹⁵ Zingg, D. W., “Comparison of High-Accuracy Finite-Difference Methods for Linear Wave Propagation,” *SIAM J. Sci. Comput.*, Vol. 22, No. 2, 2000, pp. 476–502.
- ¹⁶ Astley, R. J., “Numerical Methods for Noise Propagation in Moving Flows, with Application to Turbofan Engines,” *Acoust. Sci. & Tech.*, Vol. 30, 2009, pp. 227–239.
- ¹⁷ Rienstra, S. W., “A Classification of Duct Modes based on Surface Waves,” *Wave Motion*, Vol. 37, 2003, pp. 119–135.
- ¹⁸ Brambley, E. J. and Peake, N., “Classification of Aeroacoustically Relevant Surface Modes in Cylindrical Lined Ducts,” *Wave Motion*, Vol. 43, 2006, pp. 301–310.
- ¹⁹ Brambley, E. J., “Surface Modes in Sheared Flow using the Modified Myers Boundary Condition,” AIAA paper 2011-2736, 2011.
- ²⁰ Tam, C. K. W., Ju, H., and Chien, E. W., “Scattering of Acoustic Duct Modes by Axial Liner Splices,” *J. Sound Vib.*, Vol. 310, 2008, pp. 1014–1035.
- ²¹ Tang, L. and Baeder, J. D., “Uniformly Accurate Finite Difference Schemes for p-Refinement,” *SIAM J. Sci. Comput.*, Vol. 20, No. 3, 1999, pp. 1115–1131.
- ²² Trefethen, L. N., “Group Velocity in Finite Difference Schemes,” *SIAM Review*, Vol. 24, No. 2, 1982, pp. 113–136.
- ²³ Pridmore-Brown, D. C., “Sound Propagation in a Fluid Flowing Through an Attenuating Duct,” *J. Fluid Mech.*, Vol. 4, 1958, pp. 393–406.
- ²⁴ Brambley, E. J., “A well-posed boundary condition for acoustic liners in straight ducts with flow,” *AIAA J.*, Vol. 49, No. 6, 2011, pp. 1272–1282.
- ²⁵ Karabasov, S. A. and Goloviznin, V. M., “New Efficient High-Resolution Method for Nonlinear Problems in Aeroacoustics,” *AIAA J.*, Vol. 45, No. 12, 2007, pp. 2861–2871.
- ²⁶ Karabasov, S. A. and Goloviznin, V. M., “Compact Accurately Boundary-Adjusting High-Resolution Technique for Fluid Dynamics,” *J. Comput. Phys.*, Vol. 228, 2009, pp. 7426–7451.